

MIT Open Access Articles

Shapes of river networks

The MIT Faculty has made this article openly available. **Please share** how this access benefits you. Your story matters.

Citation: Yi, Robert S. et al. "Shapes of river networks." Proceedings of the Royal Society A: Mathematical, Physical and Engineering Sciences, 474, 2215 (July 2018): 20180081 © 2018 The Author(s)

As Published: 10.1098/RSPA.2018.0081

Publisher: The Royal Society

Persistent URL: <https://hdl.handle.net/1721.1/126787>

Version: Author's final manuscript: final author's manuscript post peer review, without publisher's formatting or copy editing

Terms of use: Creative Commons Attribution 4.0 International license





Subject Areas:

xxxxx, xxxxx, xxxx

Keywords:

river basins, aridity index, Hack's law, universality, climate

Author for correspondence:

Robert Yi

e-mail: robert@ryi.me

Shapes of river networks

Robert S. Yi¹, Álvaro Arredondo¹, Eric Stansifer¹, Hansjörg Seybold² and Daniel H. Rothman¹

¹Lorenz Center, Department of Earth, Atmospheric, and Planetary Sciences, Massachusetts Institute of Technology, Cambridge, MA

²Department of Environmental Systems Sciences, ETH Zurich, Zurich, Switzerland

River network scaling laws describe how their shape varies with their size. However, the regional variation of this size-dependence remains poorly understood. Here we show that river network scaling laws vary systematically with the climatic aridity index. We find that arid basins do not change their proportions with size, while humid basins do. To explore why, we study an aspect ratio L_{\perp}/L_{\parallel} between basin width L_{\perp} and basin length L_{\parallel} . We find that the aspect ratio exhibits a dependence on climate and argue that this can be understood as a structural consequence of the confluence angle. We then find that, in humid basins, the aspect ratio decreases with basin size, which we attribute to a common hydrogeological hierarchy. Our results offer an explanation of the variability in network scaling exponents and suggest that the absence of self-similarity in humid basins can be understood as a morphological expression of subsurface processes.

1. Introduction

River networks form stunning branching patterns that repeat over many scales. In recent years, their seemingly fractal appearance has led to study in the context of simple unifying dynamics that operate independent of scale [1, 2, 3]. Perhaps the conceptually simplest of these is the random walk model introduced by Scheidegger [4], who suggested river flow direction could be approximated as a random downhill choice on a lattice. A number of other simple models have also been devised. For example, a simple loosening of the downhill condition of the Scheidegger model (a random walk on a lattice in one of eight directions, rather than two or three) produces a network with different scaling properties [5]. Similarly, a class of optimal channel network models [1, 6] suggests that river networks self-organize to an energetically optimal state, bearing qualitative similarity to avalanches and other so-called self-organized critical processes [7]. Ultimately, study of such models revealed how scaling laws delineate distinct morphological classes of river networks [1, 3, 8, 9]. However, real river dynamics and forms are often subject to a wide range of geological and environmental constraints [10] so that each river network exhibits different scaling laws according to its environment. These constraints inevitably introduce variability into network scaling laws and have stymied efforts to develop a unifying theory [1, 3, 11, 12].

Here we ask how exponents of these network scaling laws can be understood through both an environmental gradient and the simple physical models described above. We then consider how these scaling laws can be understood explicitly through study of basin shape and its dependence on local aridity and a critical length scale associated with the presence of shallow groundwater.

2. Scaling, universality, and climate

River basin scaling is frequently characterized through a canonical scaling law known as Hack's law [13], which relates the length of the longest stream in a network l to basin area a by an exponent h , known as the Hack exponent:

$$l \sim a^h. \quad (2.1)$$

Following the analysis of branching angles in [14], here we consider how an environmental gradient influences h . Namely, we calculate the aridity index over the contiguous United States, defined as $\mathcal{A} = P/\text{PET}$ [15], where P is precipitation rate and PET is potential evapotranspiration. High values of \mathcal{A} correspond to humid regions, while low values of \mathcal{A} correspond to arid regions. This calculation is described further in the Appendix A. We fit lines to data of $\log_{10} l$ against $\log_{10} a$ to obtain h for arid and humid basins, shown in Figure 1. We find that arid basins have a Hack exponent of $h \simeq 0.5$, while humid basins have $h \simeq 0.6$, suggesting that the aridity index parameterizes the scaling exponent h .

Although Hack's law is canonically used to study how basin shape changes with scale, it alone does not provide a complete picture of river network scaling [3, 16]. We must also consider the sinuosity of streams [12], which can be expressed through the relation:

$$l \sim L_{\parallel}^d, \quad (2.2)$$

where d is a scaling exponent and L_{\parallel} is the basin length. Together, d and h define a *universality class* of river networks [3, 8, 9, 16], and adherence to a particular universality class would suggest that a river network's attributes can be largely understood through an underlying mathematical model.

The behaviors of d and h with \mathcal{A} are shown in Figure 2 (a) and (b). Figure 2(c) compares $d(\mathcal{A})$ and $h(\mathcal{A})$ to those values predicted by simple mathematical models [4, 5, 9]. It appears that $(d, h) \simeq (1.04, 0.50)$ in arid environments and $(d, h) \simeq (1.09, 0.59)$ in humid environments. These exponents suggest that, relative to humid basins, river networks in arid environments are roughly self-similar, in that arid basins do not change shape with changing scale. Arid networks also

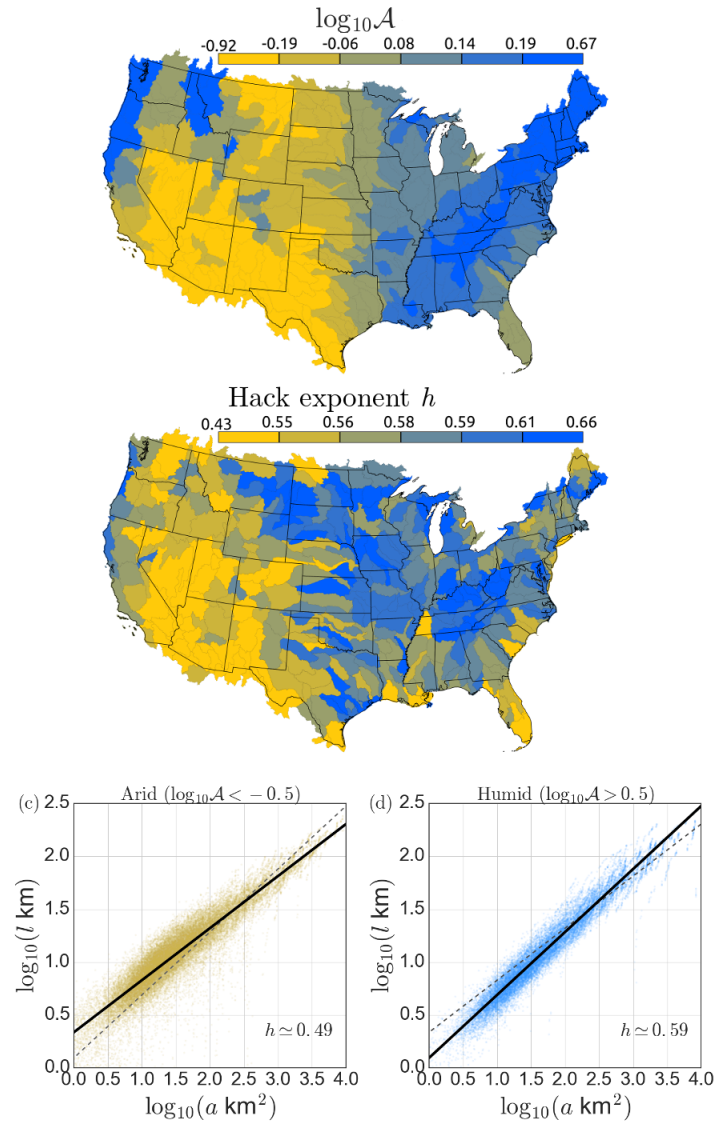


Figure 1. (a) Log aridity index $\log_{10} \mathcal{A}$ calculated for HUC6 (USGS hydrologic unit) basins in the contiguous United States. (b) Map of Hack exponent h . (c) and (d): Plots of $\log_{10} l$ vs $\log_{10} a$ for (c) arid (orange, $\log_{10} \mathcal{A} < -0.5$) and (d) humid (blue, $\log_{10} \mathcal{A} > 0.5$) regions. The black straight lines are fit to the points shown by least squares regression, and correspond to Hack exponents of $h \simeq 0.492 \pm 0.001$ for the arid data and $h \simeq 0.595 \pm 0.001$ for the humid data. The dotted grey lines indicate fits to the points shown in the opposing plot.

resemble the ground state of one of the optimal channel networks studied in [9], whereas those in humid environments do not. Still, neither the arid nor humid basins bear a definite resemblance to these universality classes of river networks. We note that the values of h and d corresponding to optimal channel networks in figure 2 are exact results deriving from global minimization of an energy functional. However, numerical simulation of optimal channel networks typically result in local minimization, yielding $h = 0.58 \pm 0.03$ [1].

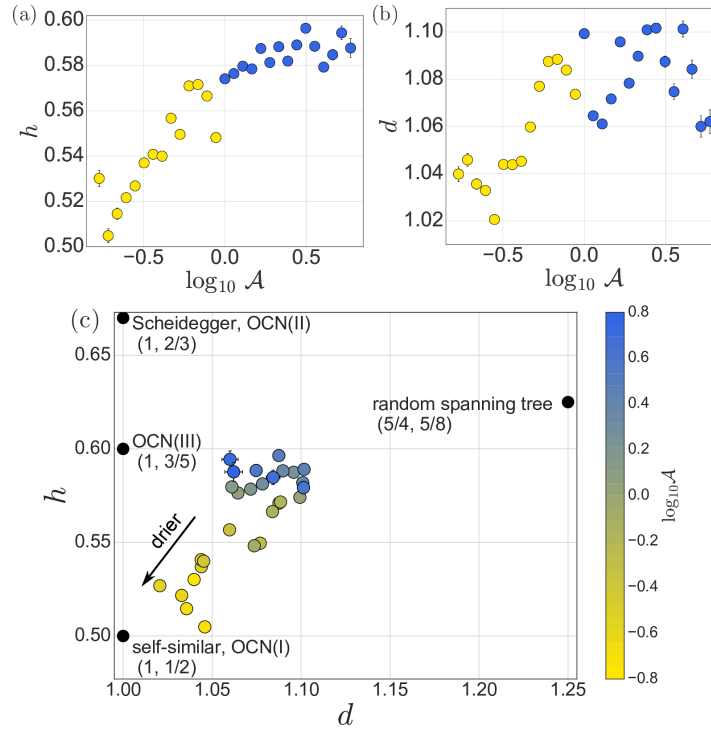


Figure 2. Behavior of (a) the Hack exponent h and (b) the sinuosity exponent d as a function of aridity index \mathcal{A} . Error bars indicate standard error. (c) Behavior of h and d , with different universality classes indicated. The four labelled black points indicate the scaling laws associated with six classic models of river networks [3]. OCN(I,II,III) are the three models of optimal channel networks analyzed in [9].

3. Basin shape

The differences in the Hack exponent h for humid and arid basins should be manifested in the size-dependence of basin shape. We therefore explicitly consider basin shape to shed light on factors that may explain the scaling behavior we have observed. We define a basin width $L_{\perp} = a/L_{\parallel}$. The aspect ratio L_{\perp}/L_{\parallel} then characterizes the shape of a basin. Figure 3(a) shows a map of L_{\perp}/L_{\parallel} . See Appendix A for a full explanation of this calculation. We find that the aspect ratio L_{\perp}/L_{\parallel} correlates with aridity, as shown in figure 3(b). In particular, basins in humid regions appear to be proportionally fatter than basins in arid regions.

To understand why, we consider how confluence angle can influence the shape of isometric basins. To this end, consider a network that can be structurally approximated as a confluence branching symmetrically with an angle α between confluent branches off of a longer parent branch, as illustrated in figure 4. We can naturally draw a boundary between two branches, and thus between the two adjacent basins, that is delineated by the direction of the parent channel. If we assume that these basins are symmetric (the area to the left of the stream is equal to the area on the right), then it follows that the drainage area a of a basin of longitudinal extent L_{\parallel} is simply a slice of angle α (radians) of a circle with radius L_{\parallel} :

$$a = \alpha L_{\parallel}^2 / 2. \quad (3.1)$$

Since $a \simeq L_{\perp} L_{\parallel}$, the aspect ratio

$$\frac{L_{\perp}}{L_{\parallel}} \simeq \frac{a}{L_{\parallel}^2} = \frac{\alpha}{2}. \quad (3.2)$$

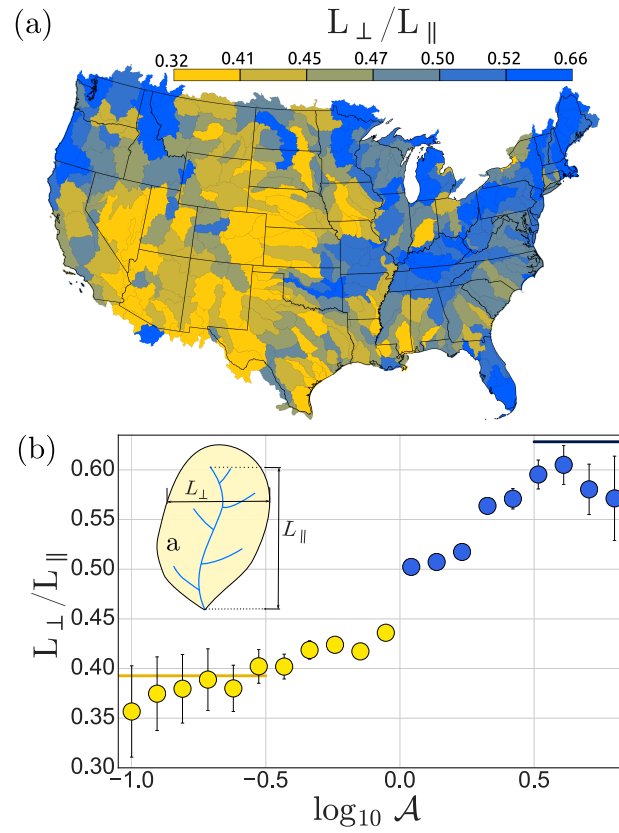


Figure 3. (a) Aspect ratio L_{\perp}/L_{\parallel} averaged for all sub-basins within each HUC6 basin over the contiguous United States. (b) Aspect ratio L_{\perp}/L_{\parallel} as a function of $\log_{10} \mathcal{A}$, with error bars indicating standard error. The yellow solid line on the bottom left of the figure indicates $L_{\perp}/L_{\parallel} = \pi/8$ and the solid dark blue line in the upper right indicates $L_{\perp}/L_{\parallel} = \pi/5$.

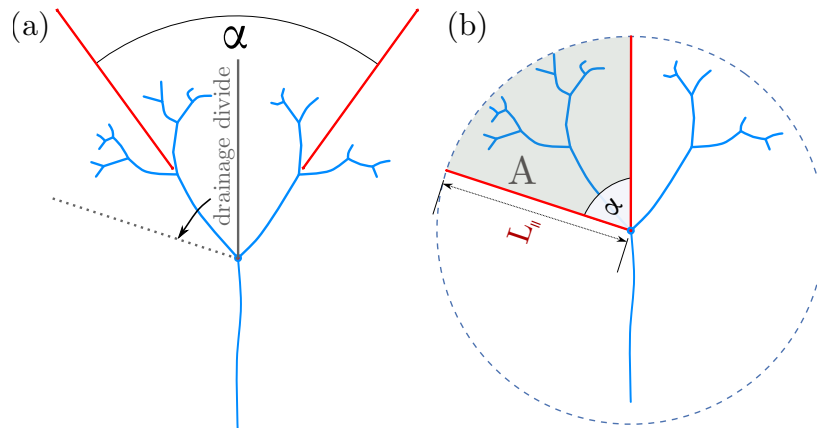


Figure 4. An illustration of how a confluence angle α might predict basin shape. (a) If the area to the left of the stream is equal to the area on the right, the drainage basin between the channels can naturally be reflected across the average stream direction. (b) If the network is then circumscribed within a circle, the basin aspect ratio can be defined as a function of branching angle.

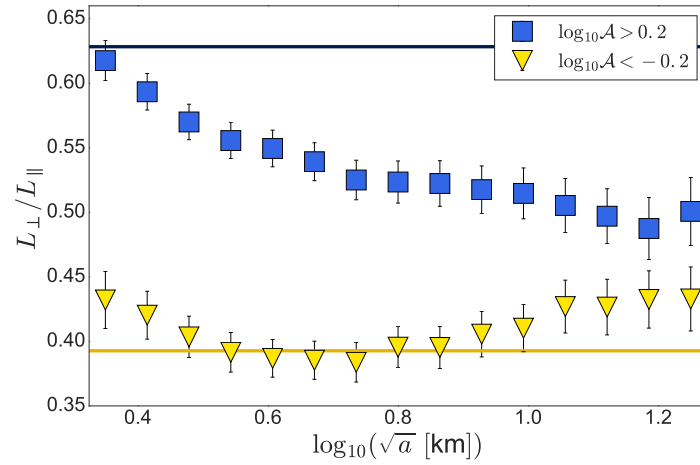


Figure 5. Dependence of aspect ratio L_{\perp}/L_{\parallel} on a . Error bars indicate standard error. The yellow line indicates an aspect ratio of $\pi/8$, and the dark blue line indicates an aspect ratio of $\pi/5$. We have relaxed the cutoffs for arid and dry regions as compared to figure 1 to include more data.

Recent work has demonstrated that groundwater-fed channel networks grow in a direction that is determined by the shape of the surrounding groundwater table, predicting a branching angle of $2\pi/5 = 72^\circ$ [17, 18]. And an analysis of the contiguous United States finds that this angle appears widespread in the local branching angles of humid environments [14], suggesting that the dynamics of groundwater processes may be influential in determining junction angle. Arid environments, however, exhibit a narrower branching angle $\sim 45^\circ$. If these two end-member branching angles are related to network-wide structures, we can predict aspect ratios for the model network of Figure 4 from the observed branching angles associated with humid and arid environments: a branching angle of 72° corresponds to $L_{\perp}/L_{\parallel} = \pi/5 = 0.63$, and a branching angle of 45° corresponds to $L_{\perp}/L_{\parallel} = \pi/8 = 0.39$. These values are indicated by solid blue and yellow lines in figure 3(b), respectively. The rough agreement suggests that the branching angles can naturally produce the observed changes in basin shape. This supports the idea that groundwater plays a substantial role in shaping river basins in humid environments.

Finally, to return to the question of variability in the Hack exponent, we consider how basin shape changes with scale. Figure 5 shows L_{\perp}/L_{\parallel} as a function of basin area a for two different aridity ranges. We find that the aspect ratio in arid regions remains $\simeq 0.4$ for basins of all sizes, indicating that in arid basins, proportions do not change with scale. However, the aspect ratio in humid regions indeed decreases as basin size increases, suggesting that their proportions do change with scale, in agreement with our measurements of the basin scaling laws in figures 1 and 2. Specifically, humid basins appear to exhibit an aspect ratio of about $\pi/5 = 0.63$ when small, but as basin size increases, there is an apparent transition towards a smaller aspect ratio of about $\pi/8 = 0.39$ characteristic of arid basins.

4. Deeper connections

We hypothesize that this scale-dependent humid basin shape may be an expression of the scale-dependence of subsurface water flow. In particular, the groundwater processes that give rise to the 72° confluence angle [17] and the $\pi/5$ aspect ratio in humid basins require nonlocal communication between branches through the groundwater field, but this interaction may be limited in its spatial extent. To understand the limiting length of subsurface interaction, we require a characterization of the groundwater table and its relationship with the topography. To this

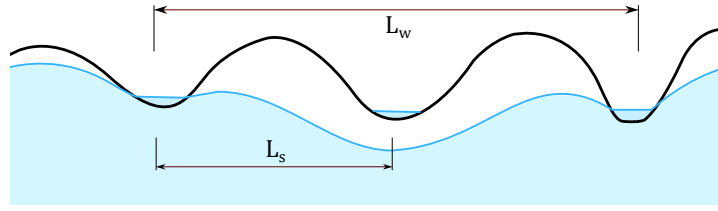


Figure 6. An illustration of the length scales L_s , the typical distance between streams, and L_w , the typical distance between streams that intersect the water table.

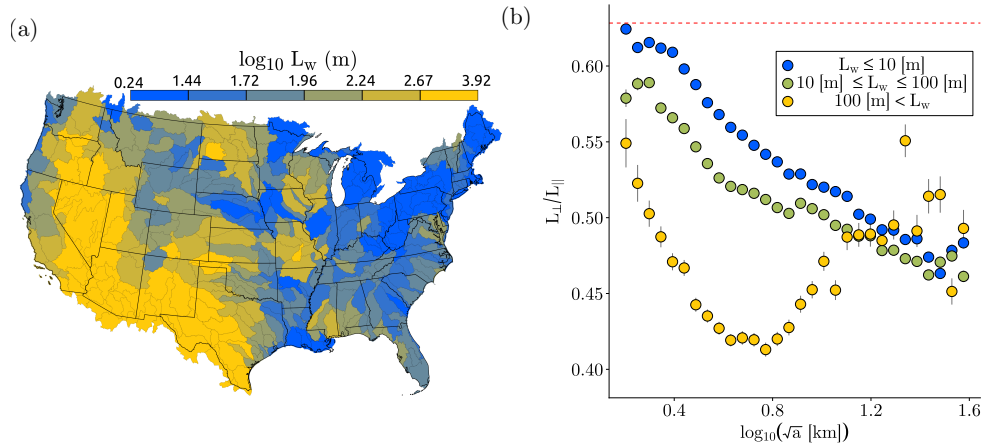


Figure 7. (a) L_w calculated for each HUC6 basin. (b) Effect of L_w and basin size on basin aspect ratio L_{\perp}/L_{\parallel} . The red dotted lines indicate the aspect ratios $\pi/5$ and $\pi/8$.

end, we consider two lengths: the typical distance L_s between streams and the typical distance L_w between streams that intersect the water table. An illustration of these length scales can be found in figure 6. By definition, $L_s \leq L_w$. When $L_s \sim L_w$, most streams present are groundwater-fed. When $L_w \gg L_s$, a number of streams form from overland flow and are decoupled from subsurface flow.

Inspired by Refs. [19, 20], we define L_w as

$$L_w = \sqrt{\frac{mkHD}{R}}, \quad (4.1)$$

where R is the recharge rate, k is the hydraulic conductivity, H is the thickness of the water table, D measures topographic relief, and m is a constant. A derivation motivating this quantity can be found in Appendix B.

We calculate L_w throughout the contiguous United States using compilations of hydraulic conductivity, recharge rate, and elevation following Ref. [20] (see Appendix A). Figure 7(a) shows the geographic distribution of L_w , and figure 7(b) shows L_{\perp}/L_{\parallel} as a function of basin size for $L_w < 10$ m (blue), $10 \text{ m} < L_w < 100$ m (green), and $L_w > 100$ m (yellow). Although we do not know the detailed geographic variation of L_s , it likely ranges between 0.1 and 1 km [21, 22]. Therefore, $L_w < 100$ m (blue) likely corresponds to $L_w \sim L_s$ and $L_w > 100$ m (yellow) likely corresponds to $L_w > L_s$. In the latter case, the water table does not intersect low-order streams. The aspect ratio of basins beyond this scale decreases to less than about 0.5, consistent with figure 5.

On the other hand, when $L_w < 100$ m, $L_w \sim L_s$ and streams are fed by groundwater. In this case, we find that the aspect ratio of small basins is $\sim \pi/5$, but it becomes smaller with increasing

basin size. Its behavior with scale can be understood through the flow regimes described by Toth [23]. On the local (and smallest) scale, the shape of the groundwater table is not strongly correlated to small fluctuations in the local topographic surface, suggesting that the growth of streams on this scale is dominated by local groundwater flow [24]. It is on this scale that planform geometry can be understood through the groundwater field [17, 25, 26]. However, on the larger, regional scale, the water table replicates the topography and the resulting flows should follow topographic gradients [19, 27]. Distant streams are still coupled by groundwater flow, but the transit times of these groundwater flows are long and the fluxes are small [28, 29]. The decay from the wide aspect ratio in Figure 7(b) is therefore gradual, not immediate.

The convergence of the humid basin aspect ratio towards the arid aspect ratio may indicate that large, humid basins self-organize in the same way as arid basins of all sizes. This convergence is consistent with earlier observations that large basins are self-similar, independent of climate and geology [30, 31].

5. Summary

We have shown that arid basins have a Hack exponent of 0.5, suggestive of a self-similar model of growth in which network proportions do not change with scale. However, humid basins do not exhibit such self-similarity, growing thinner as they grow larger. We argue that this size-dependent humid basin shape results from a physical limit to groundwater processes, and that the observed Hack exponent of $h \simeq 0.6$ is a manifestation of this limit. Remarkably, these relations are found despite the natural variability one expects in a variety of geologic settings.

Our work suggests that humid river basins exhibit a unique, mathematical dichotomy. At the scale of large basins, arid and humid networks behave alike, collecting water, perhaps doing so according to an optimality principle [1, 32]. Yet, on the smallest scale, humid basins grow in response to a diffusive groundwater field [17, 26]. In this way, the extent to which the water table is submerged below the surface determines the geometry of drainage networks at the surface.

Data Accessibility. Raw river data was obtained from NHDPlus Version 2, available at http://www.horizon-systems.com/NHDPlus/NHDPlusV2_home.php.

Authors' Contributions. R.S.Y., E.S. and D.H.R. designed research; R.S.Y., A.A.P., E.S., and D.H.R. performed research; R.S.Y., A.A.P., and H.S. analyzed data; R.S.Y. and D.H.R. wrote the paper.

Competing Interests. We declare we have no competing interests.

Funding. This material is based upon work supported by the US Department of Energy, Office of Science, Office of Basic Energy Sciences, Chemical Sciences, Geosciences and Biosciences Division under award number FG02-99ER15004.

Acknowledgements. We thank Yossi Cohen and Olivier Devauchelle for their insightful comments.

A. Appendix

We study the geometry of drainage basins across the contiguous United States, derived from the NHD Plus Version 2 data set [33]. Each drainage basin is comprised of a number of sub-basins, each with a total upstream drainage area a and longest stream length l . We find the longitudinal basin length, L_{\parallel} by taking the distance between the start and end coordinates of the longest stream. These start and end coordinates were obtained by projecting the NHDPlus stream networks onto the Lambert conformal cone 102004 projection as described in [14]. To obtain the aspect ratio L_{\perp}/L_{\parallel} , we observe that because $a \simeq L_{\perp} L_{\parallel}$, we can write this aspect ratio equivalently as a/L_{\parallel}^2 , which we then calculate for all basins and sub-basins within the contiguous United States.

We calculate the Hack exponent h in figure 2 by obtaining the slope of a line fit by least squares to $\log_{10} l$ against $\log_{10} a$. We similarly calculate the sinuosity exponent d by fitting $\log_{10} l$ against $\log_{10} L_{\parallel}$. We produce the map of h by applying the same methods to all basins geographically contained in each HUC6 basin. For all other maps, we average values within each

HUC6 basin. To determine the climatic dependence of these exponents, we calculate the aridity index $\mathcal{A} = P/\text{PET}$ [15], computed at 4 km resolution using data from PRISM [34], as in [14], then interpolate these values at the points of each stream. P is the precipitation rate, and PET is the potential evapotranspiration. Within each sub-basin, we take the geometric mean of \mathcal{A} over the entire length of all rivers in the sub-basin. For the calculation of the network scaling exponents, we used geographically diverse points which exhibited values of \mathcal{A} within the plotted bin ranges. We calculate L_w using data from Refs. [20, 35, 36, 37] following Ref. [20] and equation 4.1. We consider the topographic relief D to be the maximum terrain rise between neighboring river junctions.

B. The length scale L_w

Consider a region of terrain such that within the domain, the dominant form of water transportation is the transport of groundwater, but any groundwater that reaches the edge of the domain is drained away; call the length-scale of the domain L , such that the area of the domain is like L^2 times a small constant. A simple example of such a domain might be a circular region of radius L with no rivers on the interior but rivers along most of the outside edge.

Suppose that the height of the groundwater at each point in the domain is $H + h$, where H is a large constant, and h accounts for the (presumably small) variations of height within the domain. Then by Darcy's law, the groundwater discharge at a point is

$$k(H + h)\nabla(H + h) = k(H + h)\nabla h \approx kH\nabla h, \quad (\text{A } 1)$$

where k is the hydraulic conductivity, and ∇h is the slope in h .

By reckoning the balance between water flowing in and out of the domain, we can estimate a typical magnitude for h within the domain necessary to make the flow of water balance. The total rate at which water is added to the groundwater in the domain through rainfall is equal to the *groundwater recharge rate* R times the area of the domain. This equals the total outflow of water along the border of the domain:

$$\iint R dA = \oint kH(\nabla h \cdot \hat{n}) dl, \quad (\text{A } 2)$$

where the left integral is taken over the whole area of the domain, and the right integral is taken over the boundary of the domain and \hat{n} is the normal vector. (This is essentially Gauss's law.) If we say that R is roughly constant over the whole domain and that the magnitude of ∇h is also roughly constant along the boundary, and we ignore constants to let L^2 stand for the area of the domain and L to stand for its perimeter, we get

$$RL^2 = kH |\nabla h| L. \quad (\text{A } 3)$$

which is to say, that a typical value for the slope $|\nabla h|$ is RL/kH , times small constants. Thus the typical variation in groundwater height h over the lengthscale L of the domain is

$$\Delta h \approx \frac{RL^2}{kH}. \quad (\text{A } 4)$$

In the special case of a perfectly circular domain of radius L surrounded by water on all sides, with a recharge rate R that is constant within the whole domain, we can exactly solve the Poisson equation

$$R = -kH\nabla^2 h \quad (\text{A } 5)$$

and find that the difference of the highest value of h (in the middle) and the lowest value of h (on the border) is exactly

$$\Delta h = \frac{RL^2}{2kH}, \quad (\text{A } 6)$$

which is consistent with the estimate given above. Here the small constant is $1/2$, but in general the value will depend on the shape of the domain (smaller for less circular domains) and the fraction of the boundary which has rivers (smaller if not all of the boundary has rivers). Finally,

we identify $L_w = L$ and $D = \Delta h$ and recover equation 4.1 for the case $m = 1$ after rearrangement of equation A 4.

References

- 1 Rodríguez-Iturbe I, Rinaldo A. 2001 *Fractal river basins: chance and self-organization*. Cambridge University Press.
- 2 Tarboton D, Bras R, Rodríguez-Iturbe I. 1988 The fractal nature of river networks. *Water Resources Research* **24**, 1317–1322.
- 3 Dodds P, Rothman D. 2000 Scaling, universality, and geomorphology. *Annual Review of Earth and Planetary Sciences* **28**, 571–610.
- 4 Scheidegger A. 1967 A stochastic model for drainage patterns into an intramontane trench. *Hydrological Sciences Journal* **12**, 15–20.
- 5 Manna S, Dhar D, Majumdar S. 1992 Spanning trees in two dimensions. *Physical Review A* **46**, R4471.
- 6 Rinaldo A, Rodríguez-Iturbe I, Rigon R, Ijjasz-Vasquez E, Bras R. 1993 Self-organized fractal river networks. *Physical Review Letters* **70**, 822.
- 7 Bak P, Tang C, Wiesenfeld K. 1987 Self-organized criticality: An explanation of the $1/f$ noise. *Physical review letters* **59**, 381.
- 8 Colaiori F, Flammini A, Maritan A, Banavar J. 1997 Analytical and numerical study of optimal channel networks. *Physical Review E* **55**, 1298.
- 9 Maritan A, Colaiori F, Flammini A, Cieplak M, Banavar J. 1996 Universality classes of optimal channel networks. *Science* **272**, 984.
- 10 Bierman P, Montgomery D. 2013 *Key Concepts in Geomorphology*. W.H. Freeman.
- 11 Stankiewicz J, De Wit M. 2005 Fractal river networks of Southern Africa. *South African Journal of Geology* **108**, 333–344.
- 12 Willemijn J. 2000 Hack's law: Sinuosity, convexity, elongation. *Water resources research* **36**, 3365–3374.
- 13 Hack J. 1957 Studies of longitudinal stream profiles in Virginia and Maryland. Technical report.
- 14 Seybold H, Rothman D, Kirchner J. 2017 Climate's watermark in the geometry of stream networks. *Geophysical Research Letters* pp. n/a–n/a. 2016GL072089.
- 15 Middleton N, Thomas D. 1992 *World atlas of desertification*. United Nations Environment Programme/Edward Arnold.
- 16 Dodds P, Rothman D. 1999 Unified view of scaling laws for river networks. *Physical Review E* **59**, 4865.
- 17 Devauchelle O, Petroff A, Seybold H, Rothman D. 2012 Ramification of stream networks. *Proceedings of the National Academy of Sciences* pp. 2–6.
- 18 Cohen Y, Devauchelle O, Seybold H, Yi R, Szymczak P, Rothman D. 2015 Path selection in the growth of rivers. *Proceedings of the National Academy of Sciences* **112**, 14132–14137.
- 19 Haitjema H, Mitchell-Bruker S. 2005 Are water tables a subdued replica of the topography?. *Groundwater* **43**, 781–786.
- 20 Gleeson T, Smith L, Moosdorf N, Hartmann J, Dürr H, Manning A, van Beek L, Jellinek A. 2011 Mapping permeability over the surface of the Earth. *Geophysical Research Letters* **38**.
- 21 Montgomery DR, Dietrich WE. 1989 Source areas, drainage density, and channel initiation. *Water Resources Research* **25**, 1907–1918.
- 22 Tucker G, Catani F, Rinaldo A, Bras R. 2001 Statistical analysis of drainage density from digital terrain data. *Geomorphology* **36**, 187–202.
- 23 Toth J. 1963 A theoretical analysis of groundwater flow in small drainage basins. *Journal of geophysical research* **68**, 4795–4812.
- 24 Condon L, Maxwell R. 2015 Evaluating the relationship between topography and groundwater using outputs from a continental-scale integrated hydrology model. *Water Resources Research* **51**, 6602–6621.
- 25 Yi R, Cohen Y, Devauchelle O, Gibbins R, Seybold H, Rothman D. 2017 Symmetric rearrangement of groundwater-fed streams. *In review*.

- 26 Petroff A, Devauchelle O, Seybold H, Rothman D. 2013 Bifurcation dynamics of natural drainage networks. *Philosophical Transactions of the Royal Society of London A: Mathematical, Physical and Engineering Sciences* **371**, 20120365.
- 27 Bresciani E, Goderniaux P, Batelaan O. 2016 Hydrogeological controls of water table-land surface interactions. *Geophysical Research Letters* **43**, 9653–9661.
- 28 Cardenas M. 2007 Potential contribution of topography-driven regional groundwater flow to fractal stream chemistry: Residence time distribution analysis of Tóth flow. *Geophysical Research Letters* **34**.
- 29 Maxwell R, Condon L, Kollet S, Maher K, Haggerty R, Forrester M. 2016 The imprint of climate and geology on the residence times of groundwater. *Geophysical Research Letters* **43**, 701–708.
- 30 Mueller J. 1973 Re-evaluation of the relationship of master streams and drainage basins: Reply. *Geol. Soc. Am. Bull* **84**, 3127–3130.
- 31 Montgomery D, Dietrich W. 1992 Channel initiation and the problem of landscape scale. *Science* **255**, 826–830.
- 32 Dodds P. 2010 Optimal form of branching supply and collection networks. *Physical review letters* **104**, 048702.
- 33 McKay L, Bondelid T, Dewald T, Johnston J, Moore R, Rea A. 2012 NHDPlus Version 2: User Guide. .
- 34 PRISM Climate Group. 2012 Oregon State University. .
- 35 Wolock DM. 2003 Estimated mean annual natural ground-water recharge in the conterminous United States. Technical report.
- 36 Gleeson T, Moosdorf N, Hartmann J, Beek L. 2014 A glimpse beneath earth's surface: GLobal HYdrogeology MaPS (GLHYMPS) of permeability and porosity. *Geophysical Research Letters* **41**, 3891–3898.
- 37 for Tropical Agriculture IC Resampled SRTM version 4.1. data retrieved from CIAT, http://gisweb.ciat.cgiar.org/TRMM/SRTM_Resampled_250m/.